Supplement of Nat. Hazards Earth Syst. Sci., 18, 3297–3309, 2018
https://doi.org/10.5194/nhess-18-3297-2018-supplement

Natural Hazards and Earth System Sciences
Open Access

Supplement of

On the use of weather regimes to forecast meteorological drought over Europe

Christophe Lavaysse et al.

Correspondence to: Christophe Lavaysse (christophe.lavaysse@ird.fr)

ABSTRACT

In this supplementary materials, the methodologies employed to attribute the WRs and to assign the predictors are exposed. The different steps involved are illustrated in Fig. S1. The 500 hPa geopotential anomalies associated with each WRs are plotted in Fig. S2.

Spatial variability of the MOAWRs-SPI-1 linkages

Fig. S3 depicts these correlation values for the 16 anomalies of WR (and combination) occurrences provided by ERAI in winter and illustrates the known WR impacts on precipitation. For instance, the positive impact of the occurrence of the Atlantic Ridge (WRc) or NAO+ (WRd) on higher precipitation in the northern part of Europe, or the dry conditions associated with blocking (WRb) in north-eastern Europe (Pfahl 2014) are clearly visible.

Example of linkage between MOAWRs and observed SPI

As an example, Fig. S4 illustrates the strong linkage between the occurrence of the best WR predictor and SPI-1 over the Scandinavian Peninsula. It shows the Cumulated Distribution Function (CDF) of dry conditions (i.e. SPI-1<-1) and the reverse CDF of wet conditions (i.e. SPI-1>1) in relation to the predictors (here, the difference of occurrence between WTb and WTd). While the distribution of the predictor (distribution of WTb-WTd) is close to the normal distribution with the same number of events in both cases, the two CDFs depict a clear difference. More than 90% of dry conditions occur when the predictor is positive (i.e. more WTb than WTd during the 30-day period). The opposite is true for wet conditions. The cross-section of the two CDFs at around 0.1 is also a good indicator for evaluating the ability of the predictor to discriminate between the two conditions (i.e., its resolution, which is good if the intersection occurs close to 0 or 1, null if it is close to 0.5).

Other method of attribution tested

A second method for defining the predictors, instead of the best absolute value of correlation, was also tested using the Mixture Discriminant Analysis (MDA, Hastie and Tibshirani 1996).

This method is an extension of the linear discriminant analysis and is a classification procedure based on mixture models. Each class is assumed to be a Gaussian mixture of subclasses. This method is based on a generative model based on the posterior probability of class memberships. By weighting each parameter, each class can then be characterized. Based on the learning period and the derived parameters, the model can then predict a class in the projection period. The model parameters are estimated via an expectation-maximization algorithm. Nevertheless, due to the optimization technique, this second attribution method does not seem to be suitable for predicting extreme events as it tends to overestimate the normal conditions when the distinction is not significant. As a consequence, scores are only visible where the relationships between the WRs and the SPI-1 are the strongest and elsewhere the results remain below the benchmark (not shown). The only benefit of this overestimation of the normal condition is in the strong reduction of the FAR. For these reasons this method is not further explored in this study.

References

Hastie, T., and R. Tibshirani, 1996: Discriminant analysis by Gaussian mixtures. *Journal of the Royal Statistical Society. Series B (Methodological)*, 155–176.

Pfahl, S., 2014: Characterising the relationship between weather extremes in Europe and synoptic circulation features. *Natural Hazards and Earth System Science*, **14 (6)**, 1461–1475.

LIST OF FIGURES

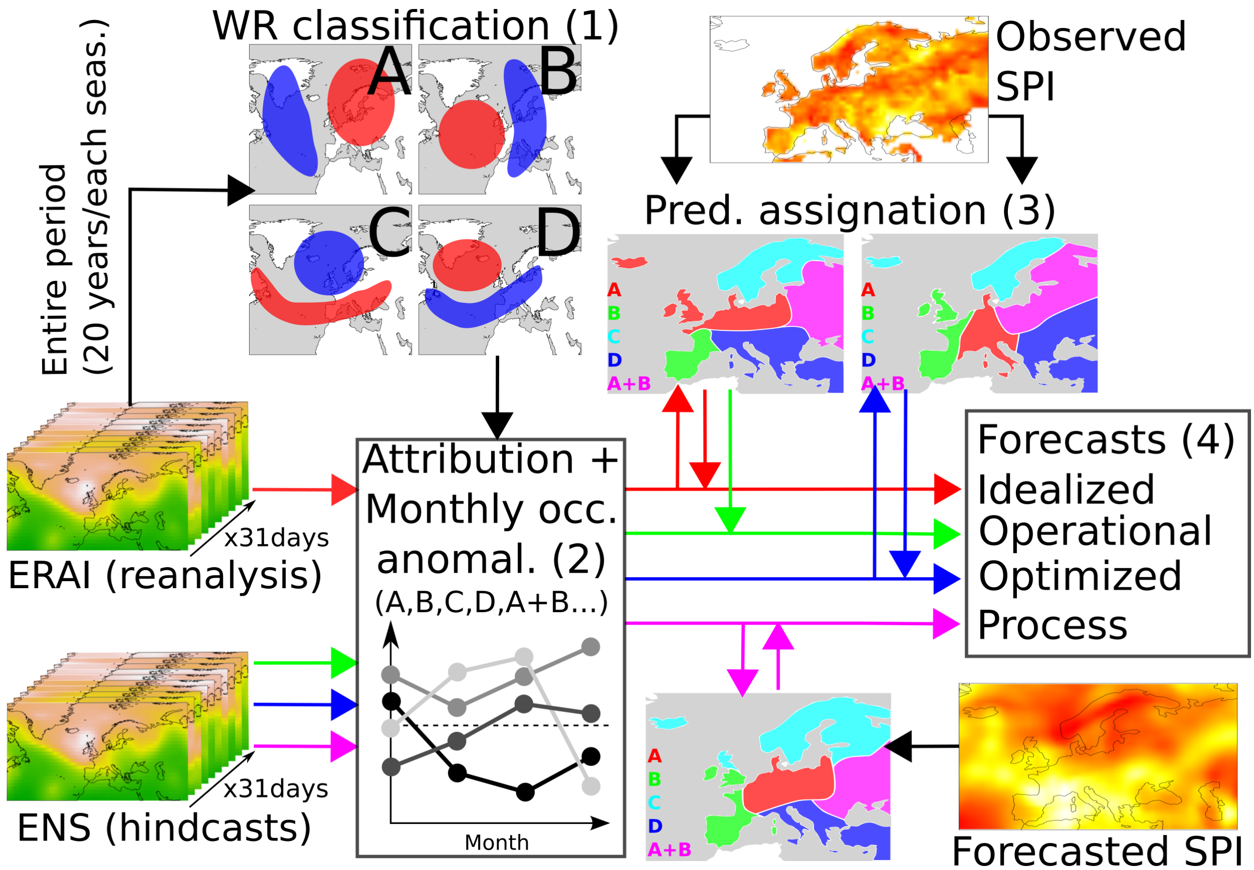

FIG. S1. Schema of the procedures to develop the forecasts by using ERAI and ENS. The process is based on three consecutive steps presented and discussed in the paper. The first one is the WR classification (1), using ERAI. The daily WR attribution (2) and the monthly occurrence anomalies are then calculated using ERAI and ENS. Finally the predictor assignations (3) are realised with 3 different combinations of correlation: i) observed precipitation and MOAWRs, ii) observed precipitation and forecasted MOAWRs, and iii) forecasted precipitation and MOAWRs. The four arrows indicate the four forecasts used in this study.

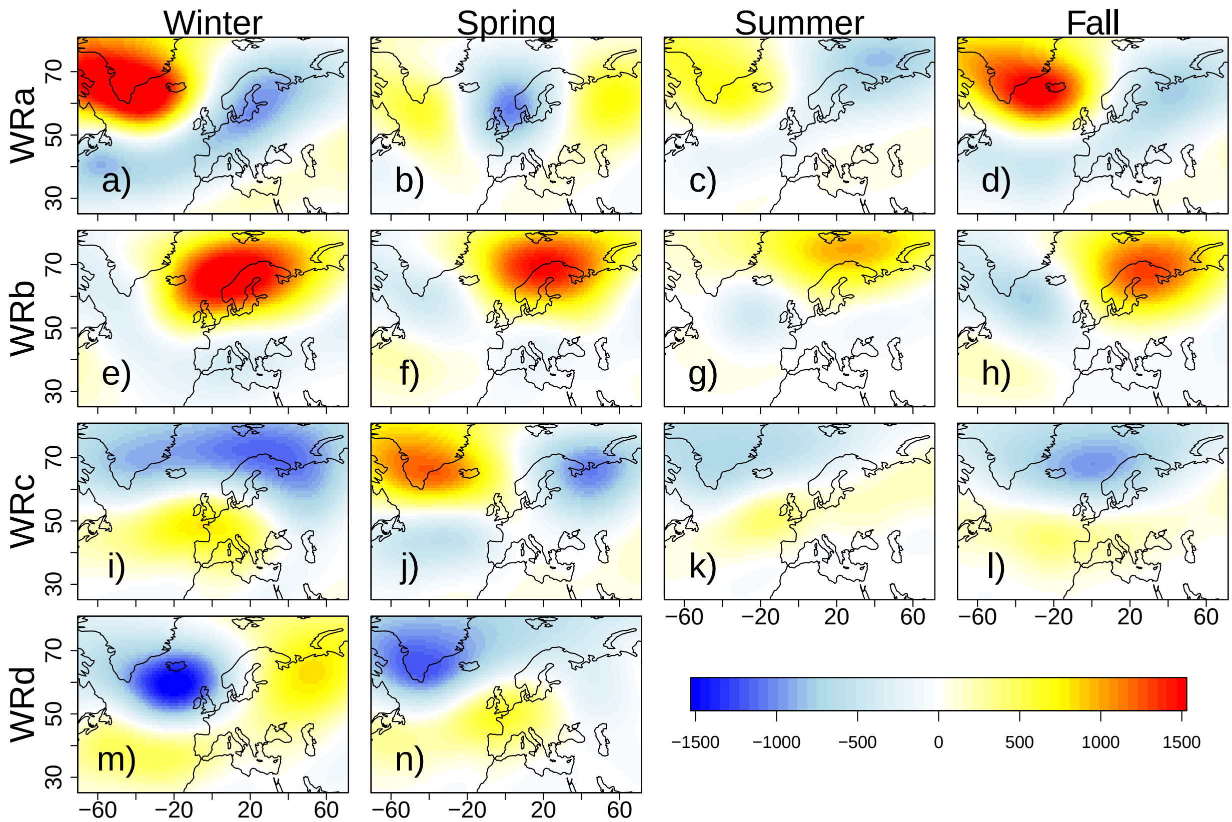

102 FIG. S2. Geopotential anomalies at 500hPa (in m) for each WR in winter (DJF), spring (MAM), summer
103 (JJA) and autumn (SON). According to the season, 3 or 4 WRs are detected using ERAI.

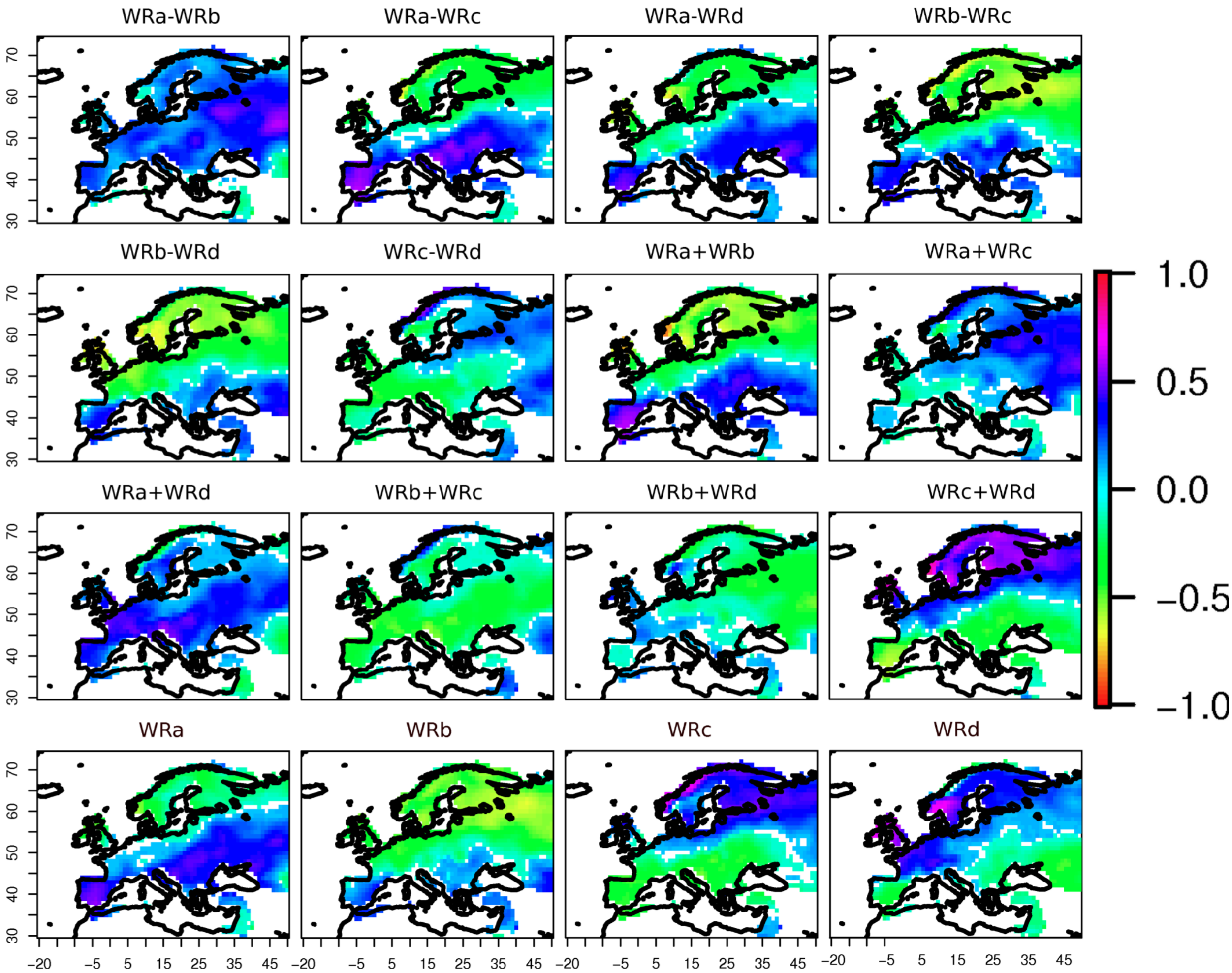

FIG. S3. Temporal correlation in winter throughout the period of hindcast between the MOAWRs and SPI-1 using the 'Idealized' or 'Operational' forecasts, i.e. observed SPI-1 and the MOAWRs derived from ERAI.

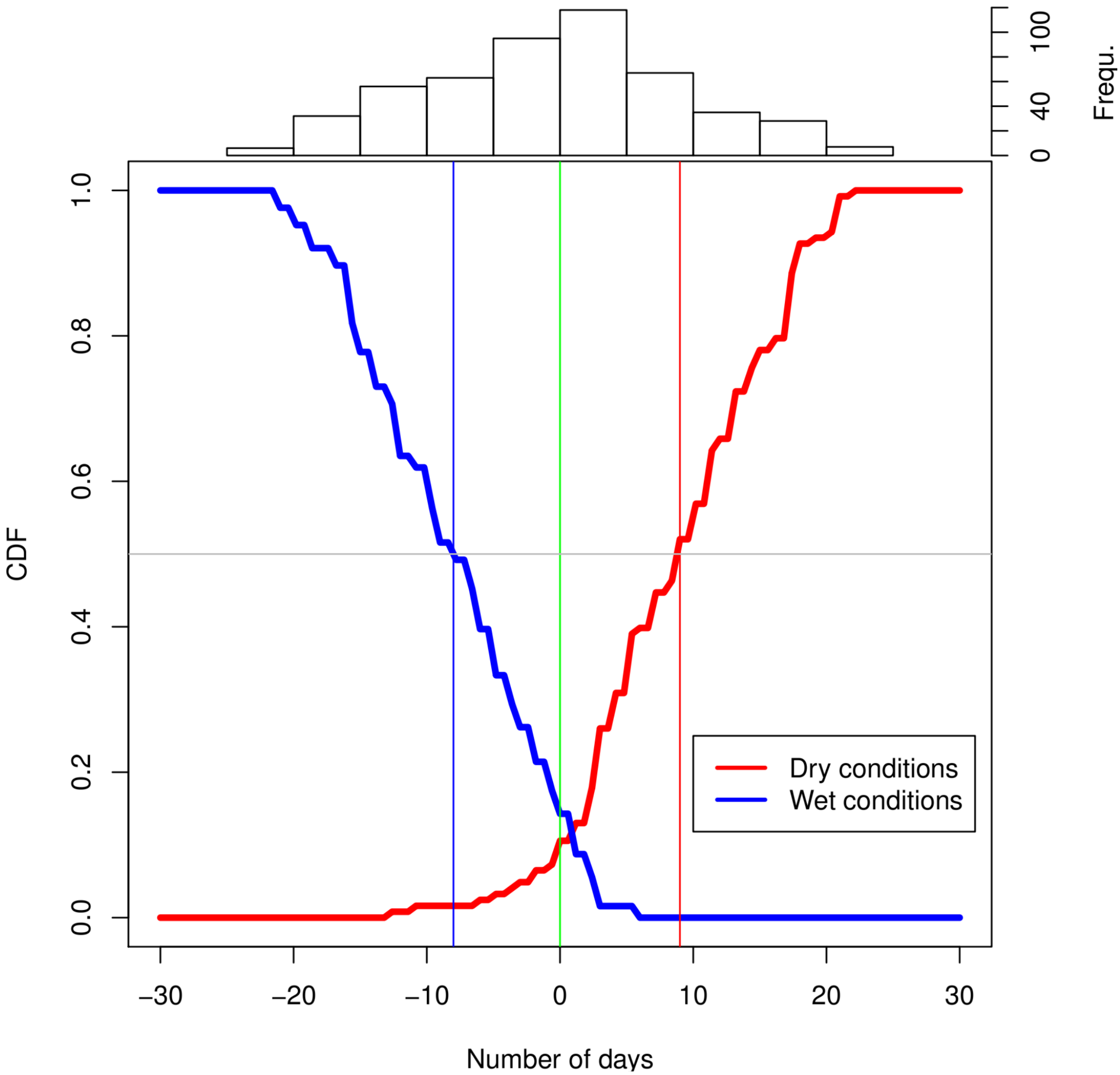

FIG. S4. Climatological distribution of cases of the predictors derived from ERAI (here, occurrence of WRb - occurrence of WRd) from -30 to 30 days (top panel). CDF of dry conditions (defined as having an observed SPI-1 lower than -1) following the predictors (red line) over the Scandinavian region. The blue line represents the inverse CDF for wet conditions (SPI-1 larger than 1). Vertical lines indicate the medians of each distribution.

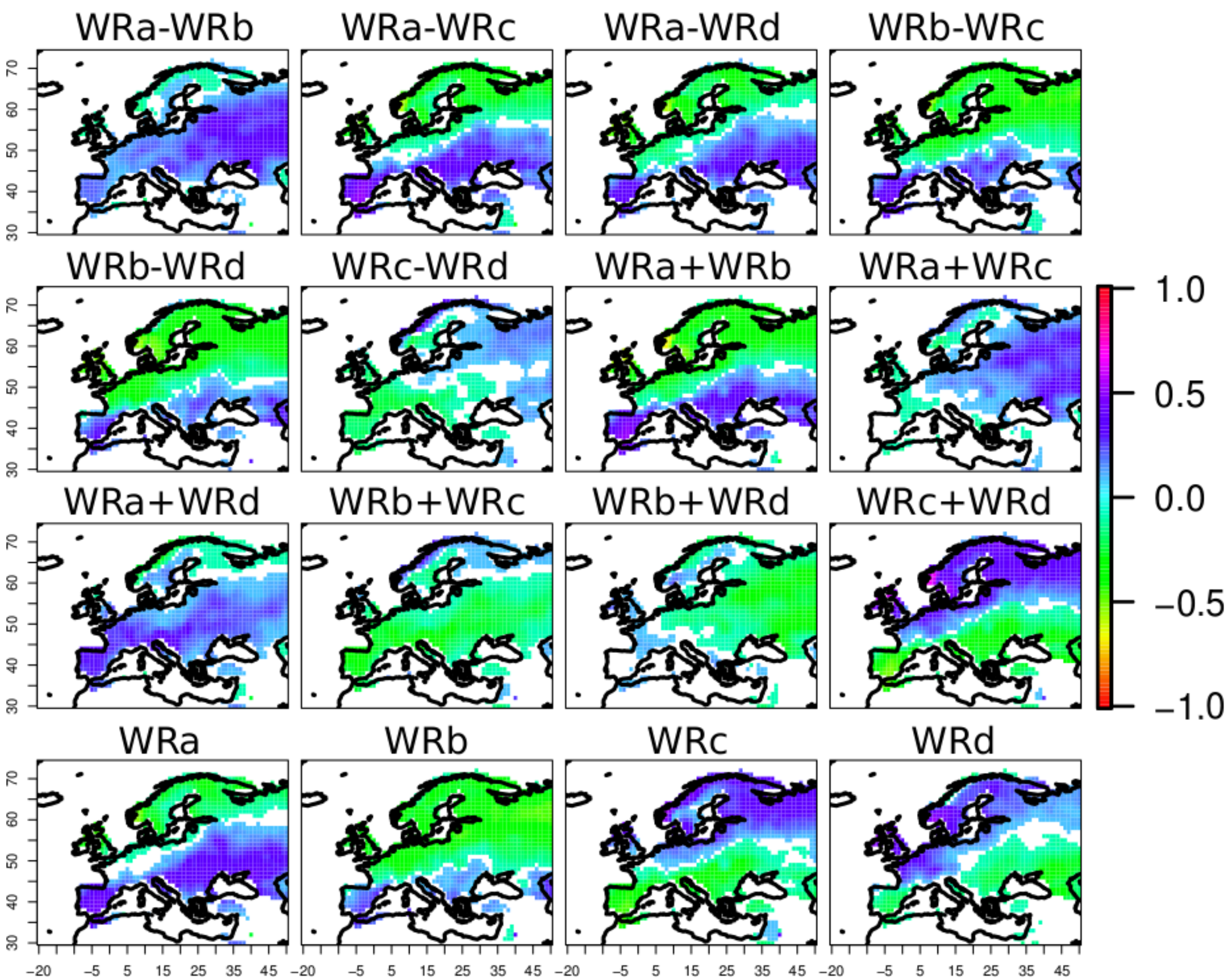

FIG. S5. Same as Fig. S3 but using the 'Optimized' forecasts, i.e. observed SPI-1 and MOAWRs derived from ENS.

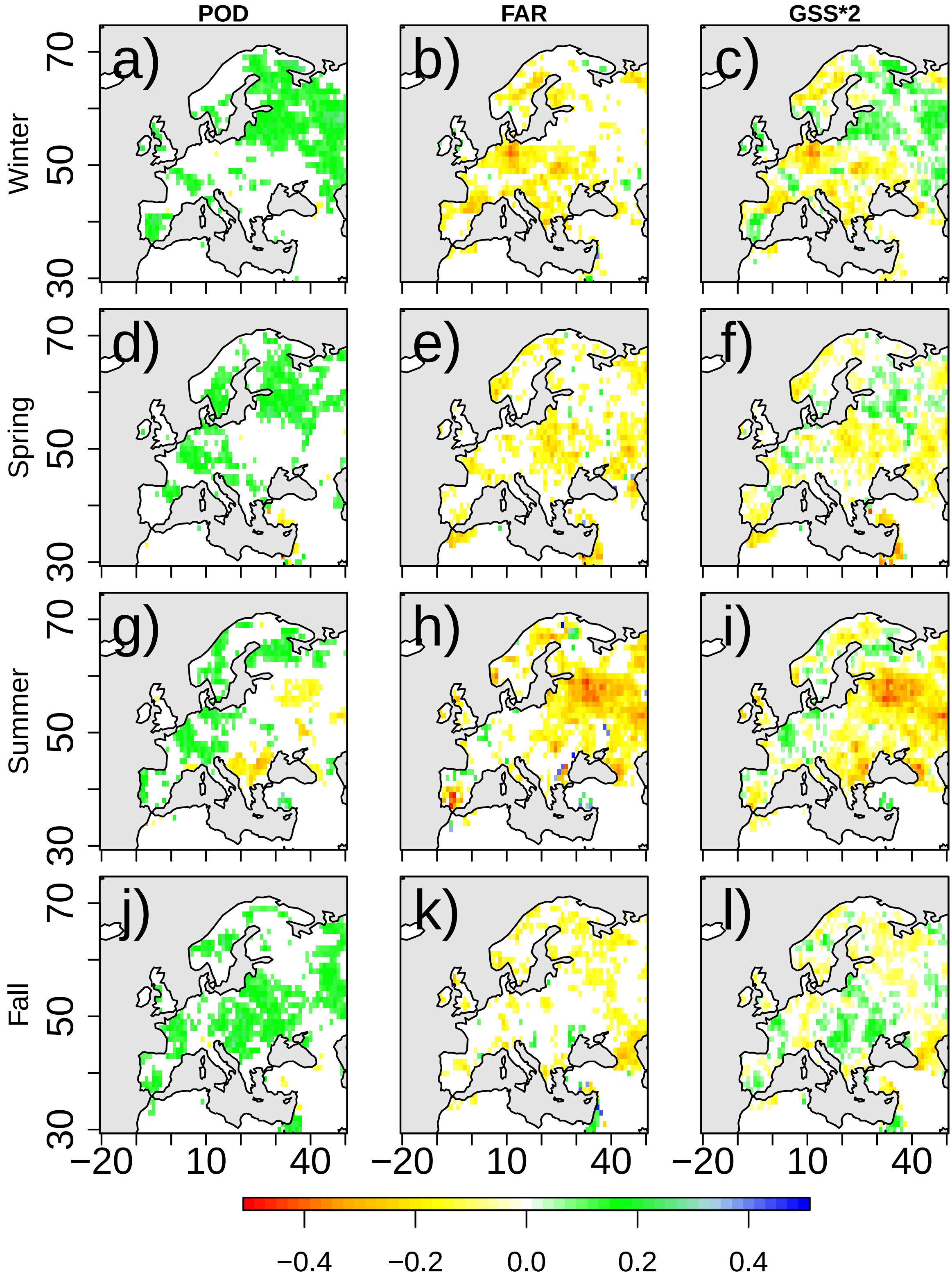

FIG. 6. Anomalies of POD (left), FAR (centre) and GSS*2 (right panels) scores of drought prediction using the 'Optimized' w.r.t. the 'Reference' forecast. The scores are calculated for (from top to bottom) winter (first), spring (second), summer (third) and autumn (fourth line).Improvement scores by using the predictors are indicated in green (inverse scale for FAR). Only difference with confidence interval larger than 90% are plotted.

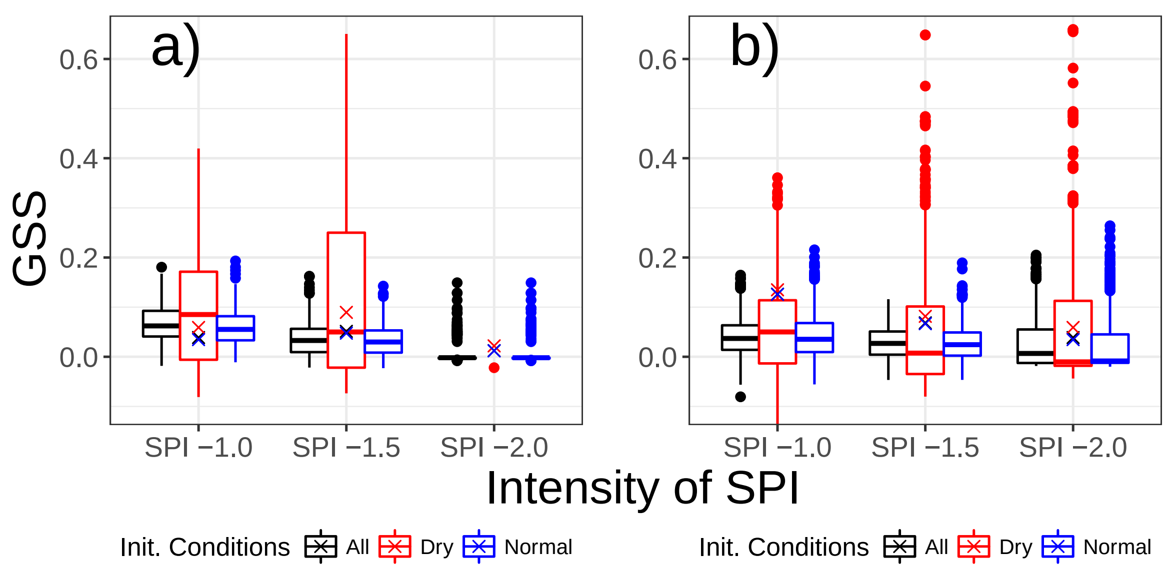

FIG. S7. Boxplot of the GSS scores in spring using the 'Reference' forecast (a) and the 'Operational' forecast (b). The scores are calculated over the entire domain and the boxes display the spatial variability. The scores are depending to the SPI intensities (-1, -1.5 and -2, x-axis) and the initial conditions defined by the previous observed SPI-2 conditions (see text for more details). Crosses indicate the scores but calculated by merging all the grid cells.

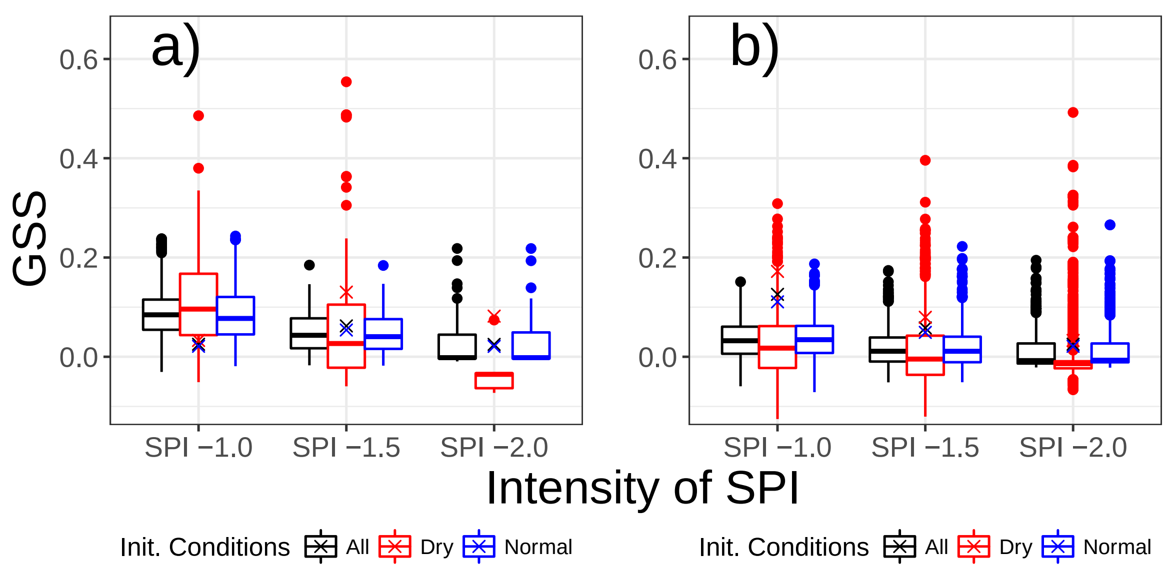

FIG. S8. Same as Fig S6 for the summer season

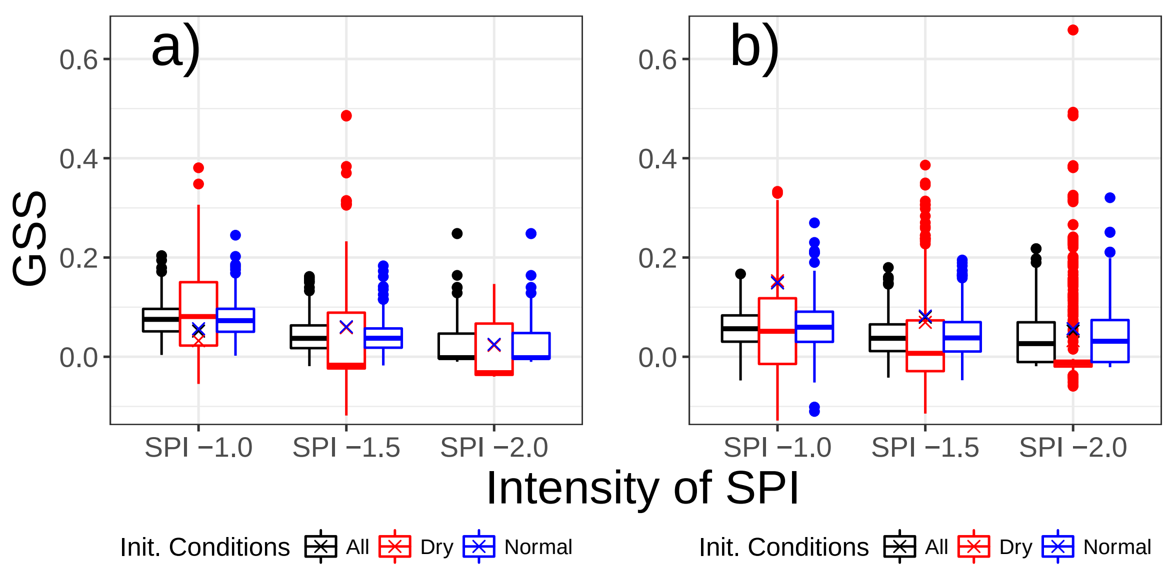

FIG. S9. Same as Fig S6 for the fall season

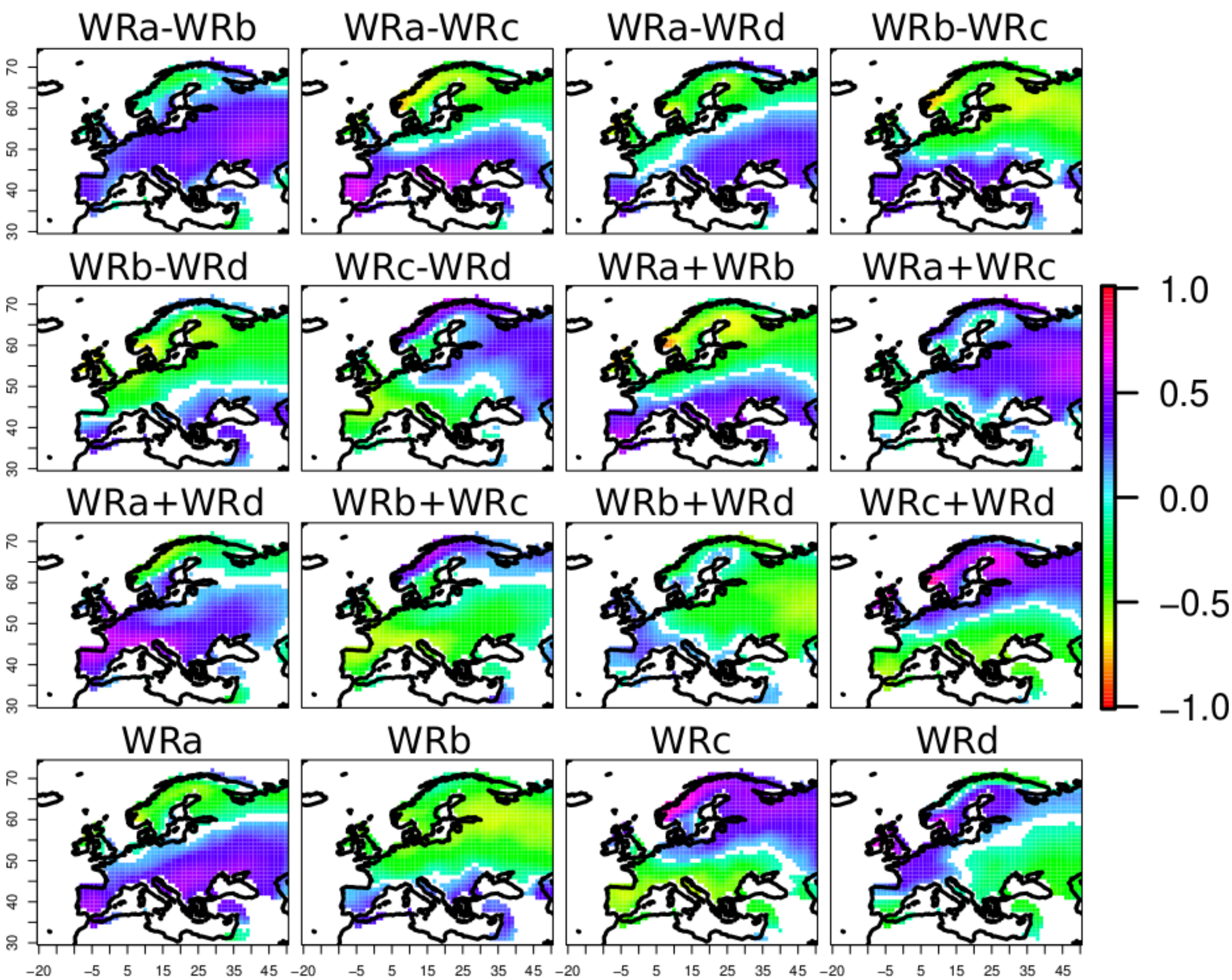

FIG. S10. Same as Fig. S3 but using the 'Process' forecasts, i.e. SPI-1 and MOAWRs derived from ENS.